Electronic Supplementary Information for:

Low-temperature activation of methane on doped single atoms: descriptor and prediction

Victor Fung,[1] Franklin (Feng) Tao,[2]* De-en Jiang[1]*

[1]Department of Chemistry, University of California, Riverside, CA 92521, USA

[2]Department of Chemical and Petroleum Engineering and Department of Chemistry, University of Kansas, Lawrence, KS 66045, USA

Corresponding Authors

*E-mail: djiang@ucr.edu; franklin.feng.tao@ku.edu

1. Supporting Figures
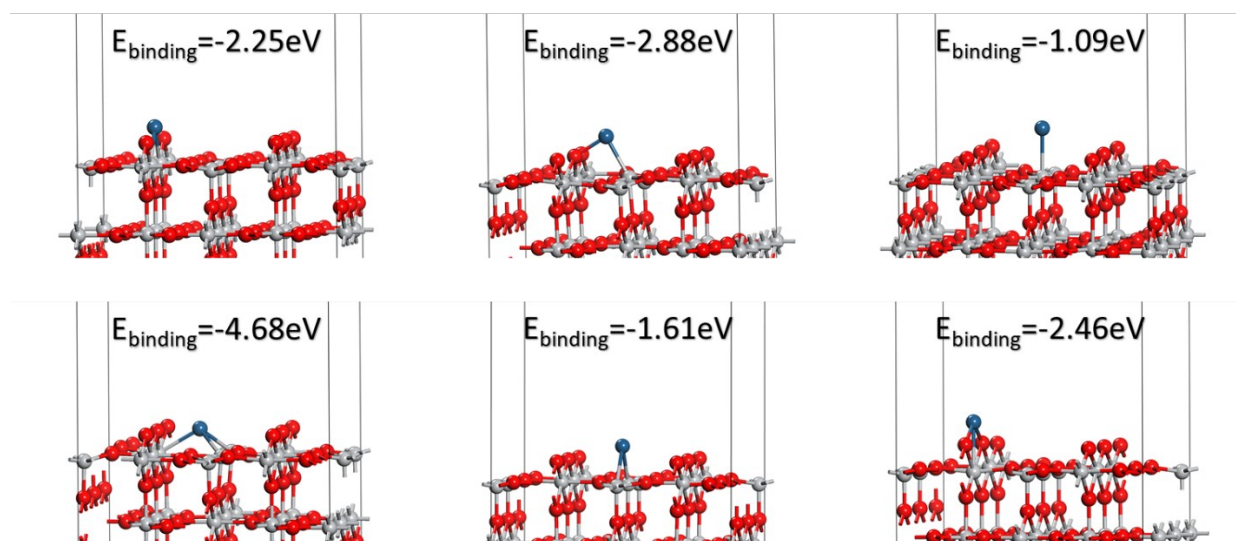
Fig. S1. Binding energies of Pt (blue) on oxygen vacancy (top left) and pristine (the rest) TiO_2 surfaces. Ti, grey; O, red.
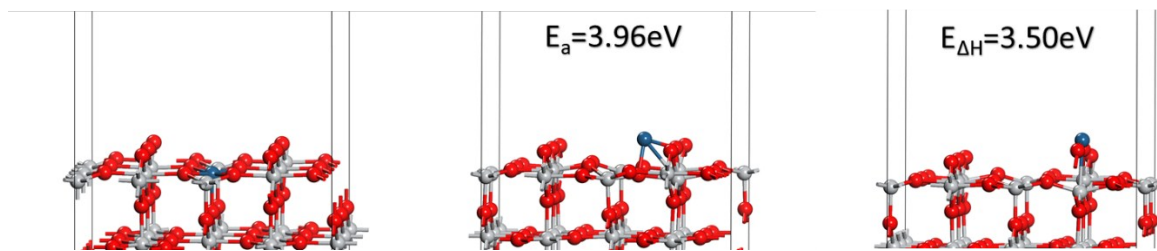
Fig. S2. Barrier and reaction energy of diffusion of Pt (blue) out of the cationic vacancy site: left, initial state; middle, transition state; right, final state. Ti, grey; O, red.
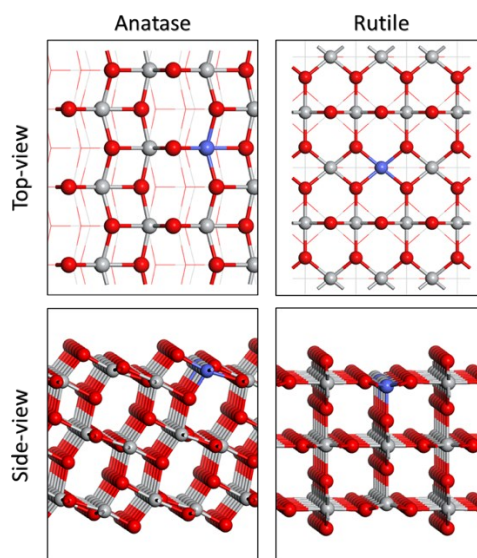

Fig. S3. Comparison of the surface doping site (highlighted in blue) on anatase (101) and rutile (110) TiO_2. Ti, grey; O, red.
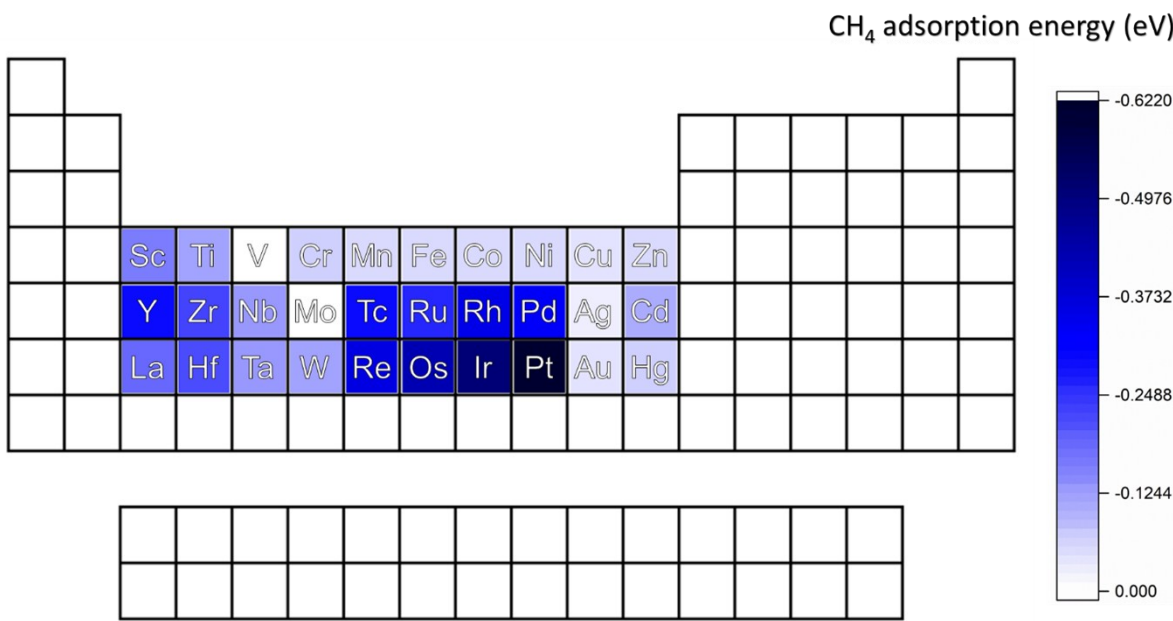
Fig. S4. Heat map representing methane adsorption energies for each transition-metal single-atom site on rutile TiO_2 (110). Darker color indicates stronger adsorption.
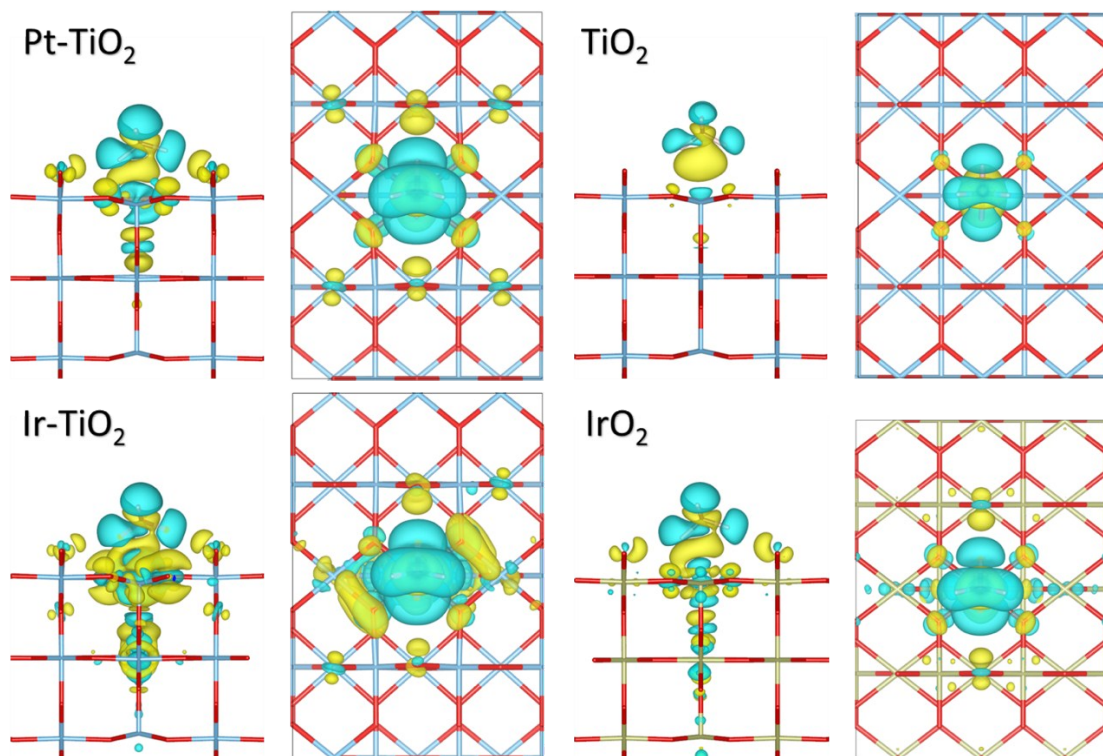
Fig. S5. Side and top-views of the isosurface plot of the charge density difference for CH_4 adsorption on rutile Pt_1-TiO_2, Ir_1-TiO_2, IrO_2, and TiO_2 (110) surfaces.
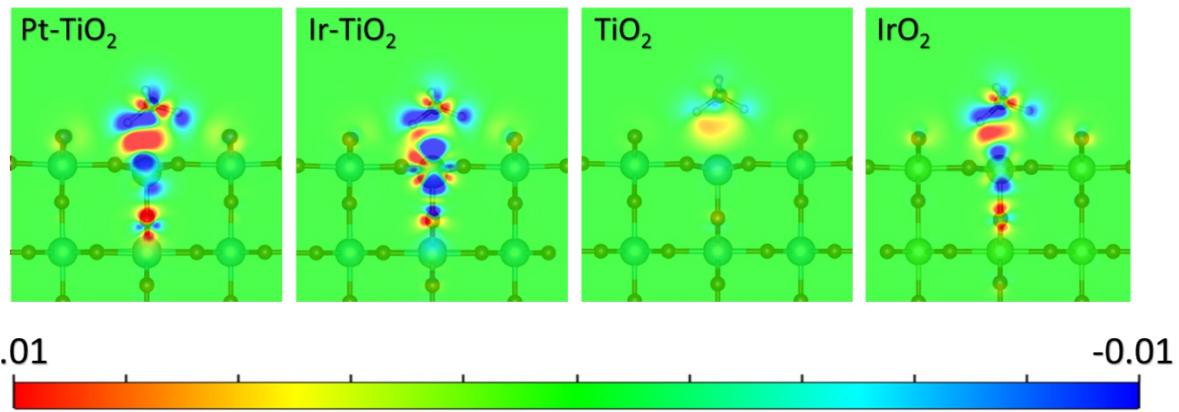
Fig. S6. Side views of the 2-D charge density plot on the H_a-C-H_b plane with charge depletion in blue and charge accumulation in red for CH_4 adsorption on rutile on rutile Pt_1-TiO_2, Ir_1-TiO_2, IrO_2, and TiO_2 (110) surfaces.
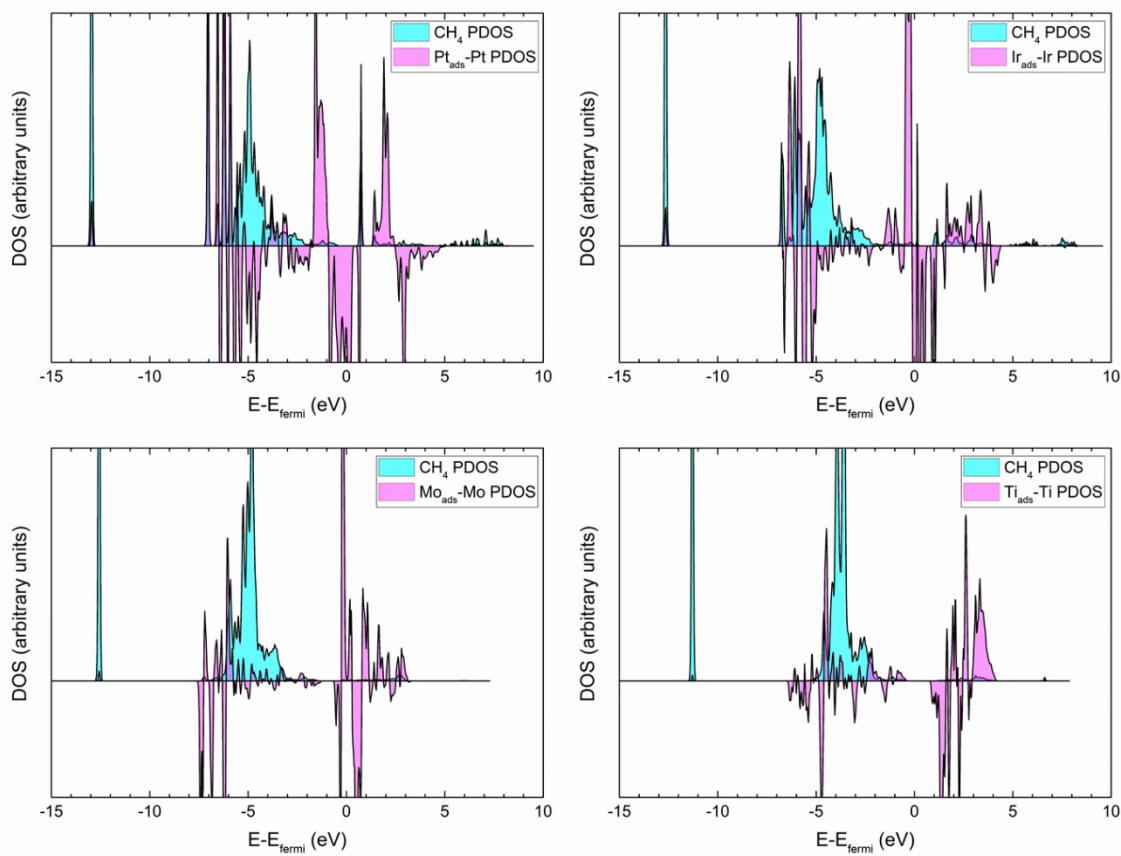
Fig. S7. Local density of states of the adsorbed CH_4 and single-atom sites for Pt_1, Ir_1, and Mo_1 on rutile TiO_2(110), in comparison with the undoped rutile TiO_2(110).

Zr, Hf^{4+} (d^0)   **Nb, Ta^{4+} (d^1)**   **Mo, W^{4+} (d^2)**   **Tc, Re^{4+} (d^3)**   **Ru, Os^{4+} (d^4)**

— dx^2-y^2 — dx^2-y^2 — dx^2-y^2 — dx^2-y^2 — dx^2-y^2

— dz^2 — dz^2 — dz^2 — dz^2 — dz^2

— dxy   — dxy   — dxy   ⇅ dxy   ⇅ dxy

— — dxz dyz   ↿ — dxz dyz   ↿ ↿ dxz dyz   ↿ ↿ dxz dyz   ↿⇂ ↿ dxz dyz

Rh, Ir^{4+} (d^5)   **Pd, Pt^{4+} (d^6)**   **Ag, Au^{4+} (d^7)**   **Cd, Hg^{4+} (d^8)**

— dx^2-y^2 — dx^2-y^2 — dx^2-y^2 — dx^2-y^2

— dz^2 — dz^2 ↿ dz^2 ↿⇂ dz^2

↿ dxy   ↿⇂ dxy   ↿⇂ dxy   ↿⇂ dxy

↿⇂ ↿⇂ dxz dyz   ↿⇂ ↿⇂ dxz dyz   ↿⇂ ↿⇂ dxz dyz   ↿⇂ ↿⇂ dxz dyz
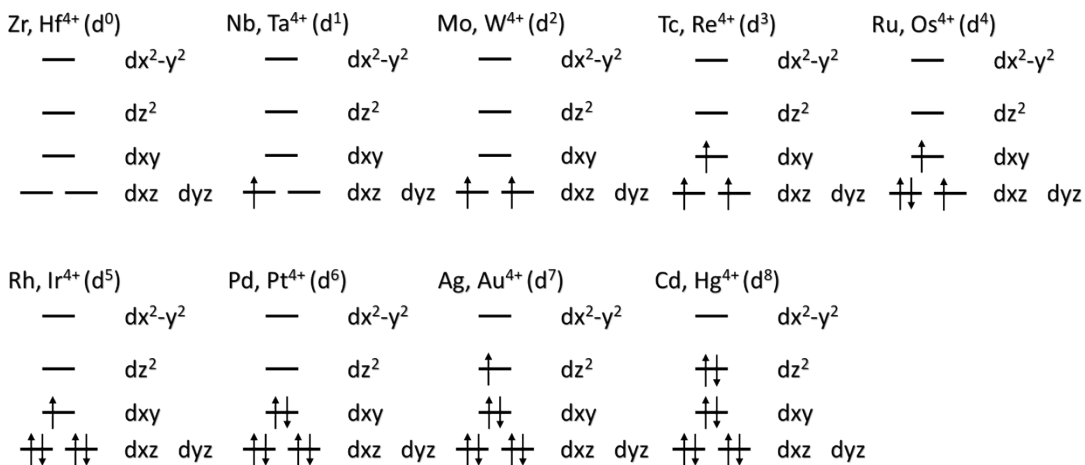
Fig. S8. Diagram of most plausible d-orbital occupations of the 4-d and 5-d transition metal single atoms on rutile TiO$_2$(110), based on the 4+ oxidation state and computationally obtained electron magnetic moments for the single atoms.

A
y=-0.09x+1.10
R^2=0.85
RMSD=0.01

C-H distance (Å)

CH$_4$ adsorption energy (eV)

B
y=1.29x+3.10
R^2=0.64
RMSD=0.16

C-M distance (Å)

CH$_4$ adsorption energy (eV)
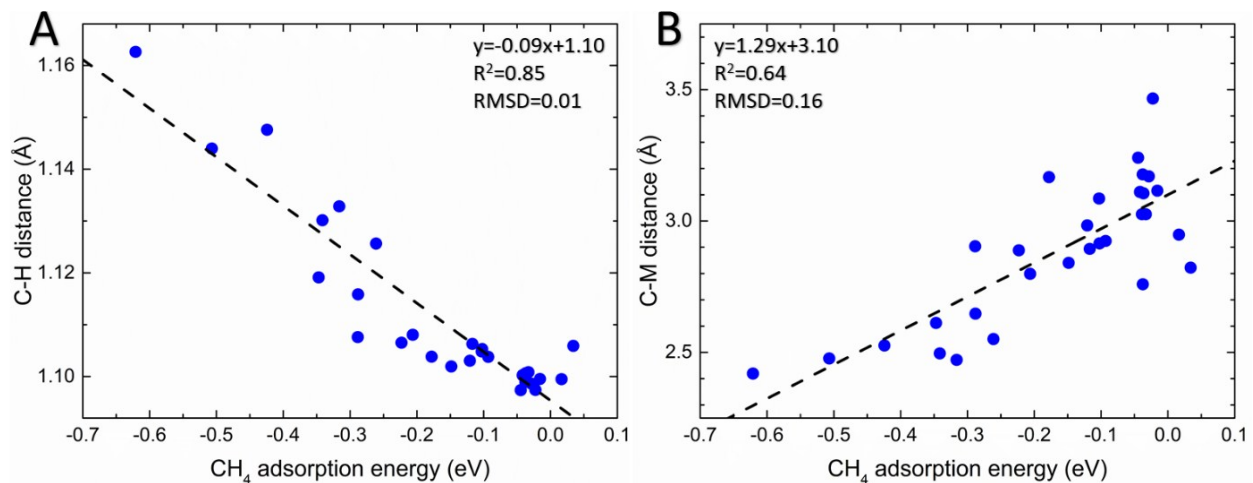
Fig. S9. CH$_4$ adsorption on the M$_1$ (single atom) site on rutile TiO$_2$ (110) for M being various transition metals: (**A**) Correlation between C-H$_a$ bond distance and CH$_4$ adsorption energy; (**B**) Correlation between C-M$_1$ distance and CH$_4$ adsorption energy. See Table S3 for the specifics of all data points.

2. Supporting Tables

**Table S1.** Binding energies of the dopant atoms into the cationic vacancy of TiO_2.

Dopant	$E_{binding}$ (eV)
Ti	-18.63
Ru	-15.64
Rh	-14.15
Pd	-10.99
Os	-16.64
Ir	-15.15
Pt	-12.95

Table S2. Comparison of CH_4 adsorption energies on the M_1 single-atom site on TiO_2 anatase (101) and rutile (110).

M_1	CH_4 ads. (eV)	
	Anatase	Rutile
Fe	-0.02	-0.04
Co	0.00	-0.04
Ni	-0.02	-0.03
Ru	-0.14	-0.26
Rh	-0.18	-0.34
Pd	-0.08	-0.32
Os	-0.21	-0.42
Ir	-0.31	-0.51
Pt	-0.18	-0.62

Table S3. Energetic and geometric parameters of methane adsorption on the M_1 single-atom site on rutile $TiO_2(110)$.

M_1	CH_4 ads. E (eV)	C-M dis. (Å)	O-H_a dis. (Å)	O-H_b dis. (Å)	C-H_a dis. (Å)	C-H_b dis. (Å)	C-H diss. E (eV)	C-H act. E (eV)	Apparent act. E (eV)
Sc	-0.15	2.841	2.577	2.551	1.102	1.106	-0.44		
Ti (undoped)	-0.10	2.915	2.650	2.492	1.105	1.102	-0.02	0.87	0.76
V	0.02	2.948	2.620	2.458	1.099	1.097	0.00	0.96	0.97
Cr	-0.04	3.111	2.662	2.563	1.100	1.101	-0.37	0.81	0.77
Mn	-0.04	2.759	2.591	2.388	1.100	1.107	-1.08	0.52	0.48
Fe	-0.04	3.106	2.723	2.640	1.101	1.098	-0.35	1.06	1.03
Co	-0.04	3.177	2.740	2.644	1.099	1.100	-1.21	0.74	0.70
Ni	-0.03	3.026	2.702	2.591	1.101	1.098	-1.82	0.52	0.49
Cu	-0.03	3.170	2.817	2.866	1.099	1.101	-1.03		
Zn	-0.04	3.026	2.713	2.691	1.100	1.103	-0.56		
Y	-0.29	2.904	2.772	2.596	1.108	1.105	-0.47		
Zr	-0.22	2.888	2.602	2.515	1.107	1.106	0.22	0.80	0.58
Nb	-0.12	2.983	2.622	2.557	1.103	1.102	-0.12	0.88	0.76
Mo	0.03	2.822	2.557	2.474	1.106	1.106	-0.36	0.69	0.72
Tc	-0.29	2.647	2.520	2.375	1.116	1.105	-0.83	0.51	0.22
Ru	-0.26	2.551	2.546	2.310	1.126	1.101	-1.23	0.38	0.12
Rh	-0.34	2.496	2.538	2.277	1.130	1.102	-1.60	0.27	-0.07
Pd	-0.32	2.471	2.527	2.275	1.133	1.103	-2.28	0.13	-0.18
Ag	-0.02	3.115	2.907	2.860	1.100	1.103	-0.88		
Cd	-0.09	2.924	2.852	2.786	1.104	1.102	-0.42		
La	-0.18	3.167	3.270	3.161	1.104	1.101	-0.36		
Hf	-0.21	2.799	2.531	2.463	1.108	1.108	0.26	0.80	0.60
Ta	-0.12	2.894	2.583	2.515	1.106	1.104	-0.23	0.78	0.66
W	-0.10	3.085	2.689	2.605	1.105	1.101	-0.49	0.70	0.59
Re	-0.35	2.612	2.522	2.334	1.119	1.107	-0.83	0.47	0.12
Os	-0.42	2.526	2.568	2.277	1.148	1.099	-1.24	0.37	-0.05
Ir	-0.51	2.477	2.524	2.269	1.144	1.100	-1.63	0.23	-0.27
Pt	-0.62	2.419	2.535	2.212	1.163	1.100	-2.24	0.15	-0.47
Au	-0.02	3.466	3.185	3.093	1.097	1.099	-0.93		
Hg	-0.04	3.241	3.028	2.968	1.097	1.101	-0.34		

Table S4. Adsorption energy of methane to some isolated, neutral gas-phase metal single atoms.

Atom	$E_{adsorption}$(eV)
Os	-0.11
Ir	-0.23
Pt	-0.13
Au	-0.01

Table S5. Bader charges (in $|e|$) prior to and after adsorption of CH_4 on rutile IrO_2(110), TiO_2(110), and Ir_1-TiO_2(110), and Pt_1-TiO_2(110).

Pre-adsorption	M_1	O_a	O_b	C	H_a	H_b
CH_4				-0.064	0.016	0.016
Rutile IrO_2	1.459	-0.707	-0.707			
Rutile TiO_2	2.026	-0.906	-0.906			
Ir_1-TiO_2	1.599	-0.904	-0.904			
Pt_1-TiO_2	1.453	-0.904	-0.904			
Post-adsorption						
Rutile IrO_2	1.465	-0.731	-0.733	-0.200	0.026	0.135
Rutile TiO_2	2.033	-0.918	-0.920	-0.151	0.030	0.070
Ir_1-TiO_2	1.558	-0.929	-0.931	-0.246	0.064	0.163
Pt_1-TiO_2	1.421	-0.933	-0.937	-0.222	0.073	0.204
Difference						
Rutile IrO_2	0.006	-0.024	-0.026	-0.136	0.010	0.119
Rutile TiO_2	0.006	-0.012	-0.015	-0.087	0.014	0.054
Ir_1-TiO_2	-0.041	-0.025	-0.027	-0.182	0.048	0.147
Pt_1-TiO_2	-0.032	-0.029	-0.033	-0.158	0.057	0.188

Table S6. Comparison of methane adsorption energy (E_{ads}), activation-energy (E_a), and dissociation energy (ΔE) on rutile TiO_2(110), and Ir_1-TiO_2(110), and Pt_1-TiO_2(110) for different functionals.

Functional	Energetics	TiO_2	Ir_1-TiO_2	Pt_1-TiO_2
PBE	E_{ads}	-0.10	-0.51	-0.62
	E_a	0.87	0.23	0.15
	ΔE	-0.02	-1.63	-2.24
PBE-D3	E_{Ads}	-0.39	-0.83	-0.95
	E_a	0.82	0.21	0.13
	ΔE	-0.05	-1.60	-2.22
optPBE-vdW	E_{Ads}	-0.37	-0.75	-0.84
	E_a	0.95	0.30	0.19
	ΔE	-0.04	-1.64	-2.27
SCAN	E_{ads}	-0.04	-0.76	-0.96
	E_a*	0.96	0.28	0.19
	ΔE	0.19	-1.68	-2.28
HSE06*	E_{ads}	-0.28	-0.48	-0.92
	E_a	1.03	0.12	0.25
	ΔE	-0.09	-2.09	-2.48

*Single point energies.